JOURNAL OF CATALYSIS 50, 43–55 (1977)

Simultaneous Electronic and Ionic Surface Conduction of Catalyst Supports: A General Mechanism for Spillover

The Role of Water in the Pd-Catalyzed Hydrogenation of a Carbon Surface

E. KEREN[1] AND A. SOFFER[2]

Department of Chemistry, Nuclear Research Center, Negev, P.O. Box 9001, Beer-Sheva, Israel

Received August 11, 1976

The experimental evidence on hydrogen spillover from catalyst to support is briefly reviewed. A double-layer charging mechanism for spillover in the solid–gas system is suggested by a gradual experimental shift from an ordinary electrode–liquid electrolyte system to a solid–gas one. The mechanism is essentially dissociation of H_2 on the catalyst to $H^+ + e$. Both species migrate onto the support surface by means of protonic and electronic conduction which must be exhibited by the support. The protonic conduction is the property of a surface electrolyte composed of surface OH and adsorbed hydrogen bonding molecules. The driving force for the observed fast migration is the electrochemical potential gradient. The observed long-range spillover, together with low-coverage saturation effects, are explained by the proposed mechanism. The main rate-determining steps for spillover are shown to be (a) H_2 dissociation to $H^+ + e$ on the catalyst surface; (b) transfer of electronic charge through the contact between catalyst and support particles; (c, d) electronic and protonic conductance.

INTRODUCTION

It has recently been understood that many supports of heterogeneous catalyst systems play some chemical role in catalysis, in addition to physical functions such as providing high dispersion and surface area for the catalyst. None of these aspects has had as much attention as the active hydrogen migration (spillover) from hydrogenation catalysts to supports. This phenomenon, which was first proposed by Sinfelt and Lucchesi (*1*) in connection with enhanced hydrogenation of ethylene upon addition of alumina to Pt–SiO_2 catalyst, has since been found on many different solids. Among them are high-surface carbon (*2–4*), WO_3 (*5, 6*), MoO_3, Fe_2O_3, and Fe_3O_4 (*7*), CuO (*8, 9*), NiO (*9*), V_2O_5 (*10, 11, 13*), UO_3 (*11–13*), Co_3O_4, Ni_3O_4, and MnO_2 (*13*).

Last but not least, hydrogen spillover has recently been reported on a specific type of partially methoxylated alumina (*14*). Sermon and Bond (*15*) give some further examples, many of them [Table 2, Ref. (*15*)] ambiguous since, as noted by the above authors (*15*), the experimental observations could also be interpreted in terms of high chemisorption stoichiometry.

In spite of the extensive more or less reliable experimental evidence of hydrogen spillover, the mechanistic aspects have received only a little attention. In this paper our aim is to try to contribute some more in this respect.

There is general agreement that molecular hydrogen is dissociated to an active mobile species which migrates onto the support. There is also no doubt that ac-

---

[1] Present address: Department of Physics, Weizmann Institute of Science, Rehovot, Israel.

[2] To whom correspondence should be addressed.

ISSN 0021-9517

ceptor sites are provided by the support. The remaining problem is the nature of the "active species" and its mechanism of diffusion.

Such a problem has been solved for two particular cases by Ekstrom *et al.* (*12*) and Batley *et al.* (*13*). They proved that, at a suitable temperature (400°C), hydrogen atoms from a $Pt–Al_2O_3$ catalyst diffuse through the gas to a *separate* UO_3 pellet, which is then reduced to UO_2, showing a visible color change. They concluded that gas diffusion is significant only at temperatures above 350°C. They also observed oxygen atom diffusion through the gaseous phase to a UF_4 pellet at 640°C which was oxidized to UO_2F_2.

In most reports on hydrogen spillover, the experimental temperatures are below 300°C and very frequently room temperature. This still leaves open the questions of the nature of the diffusing species and the mechanism of migration.

At first glance, it seems that mobile chemisorbed atomic hydrogen is a migrating species common to various spillover systems, as was suggested by Robell *et al.* (*2*) for spillover on Graphon (a graphitized carbon black). Later, they found (*3*) that, if the black was treated in hydrogen at 900°C and then evacuated at room temperature, hydrogen uptake was greatly reduced. They attributed this to the destruction, at high temperatures, of some fibrous carbon bridges which connect the platinum particles with the carbon layer support particles. These bridges conduct dissociated hydrogen from the platinum to the carbon support.

Spillover can be viewed as fluid–solid (gas-support in most cases) interaction, catalyzed by another solid catalyst. This implies that the same type of interaction occurs in the absence of a catalyst at higher temperatures, as was observed in most systems exhibiting spillover (*2–5, 12, 13*). The intriguing feature of spillover as a catalytic process is that, since both the catalyst and one of the reactants are solids, the reaction occurs on the solid support *farther* from the catalyst. Therefore, migration of the second reactant, after being activated by the catalyst, is an essential step. In ordinary heterogeneous catalysts, both reactants are in the fluid state, and the reaction proceeds on the surface of the solid catalyst.

A concept of bridging intermediates was introduced by Neikam and Vannice (*16*) who found that room-temperature spillover on Na, La, and Ce Y-zeolites is enhanced by preadsorbed large aromatic or aliphatic molecules, but never by water (*16*). They were the first to introduce a spectral method for spillover investigation (*17*) and found some evidence that atomic hydrogen is the migrating species. The nature of the H acceptor was, however, quite uncertain, especially for the Na and La zeolites and even more in the case of $Pt–SeO_2$ (*18*). It seems, therefore, that more information is needed on the amount of hydrogen accommodated by the catalyst and the bridging compound.

It is of interest to refer finally to Levy and Boudart (*20*) who made a thorough study of the effect of the presence of polar molecules on hydrogen absorption by plantinized WO_3. They found that the rate of this absorption is greater if the preadsorbed "co-catalyst" has lower proton affinity, and the proton solvated by such molecules is the active species which migrates from the supported metal and reduces the oxide.

The importance of this work, in our opinion, lies in the introduction of the proton as the migrating species. However, the proton cannot leave the catalyst surface alone and diffuse into the oxide while the electron is "left behind in the metal" (*20*). Such a process would violate the macroscopic electroneutrality of the system.

Many features characteristic of solid–gas interfaces are common to electrode processes as well (*21*). We shall utilize this commonality to introduce a new electronic–protonic mechanism of hydrogen migration, by which means we will show that the spillover effect is equivalent to an electrochemical local cell action or to a generalized (*22*) double-layer charging of an electrode surface. In order to establish this mechanism, a gradual transition was made from the aqueous electrochemical to the solid–gas system. In both systems, hydrogen spillover from palladium to carbon surface will be demonstrated.

EXPERIMENTAL

Materials. Instruments for electrochemical measurements: Constant-current power supply, Electronic Measurements, Eatontown, N. J., Model C624; electrometer, Keithley, Model 610C; strip chart recorder, Hewlett–Packard, Model 7107 BM with input module 17500A.

Triple-distilled water was used for solution preparation. Sulfuric acid from Merck was Analar grade. High-purity palladium was from Koch–Light Labs., Ltd. Palladium sulfate was prepared by prolonged heating in concentrated sulfuric acid and was diluted to 2 *M* H_2SO_4, which is the working solution in the electrochemical cell. Carbon was a Merck product (No. 2186; total ash content: 0.5%). The surface area of this carbon was 870 m^2/g, as measured by the BET method. Hydrogen and nitrogen were Matheson products, ultrapure and prepurified grades, respectively. The palladium–carbon suspension for the electrochemical system was prepared *in situ* by adding a calculated amount of palladium sulfate in 2 *M* H_2SO_4 solution to a slurry of carbon in 2 *M* H_2SO_4, followed by hydrogenation at room temperature. The same technique was applied to the Pd–C used in the solid–gas system, but the powder was repeatedly filtered and washed with triple-distilled water, until conductivity was as low as 10^{-5} mho cm^{-1}. The samples were dried in a desiccator before introduction into the vacuum system. Prolonged exposure to air during treatment after hydrogenation brought the powder to the *oxidized state.*

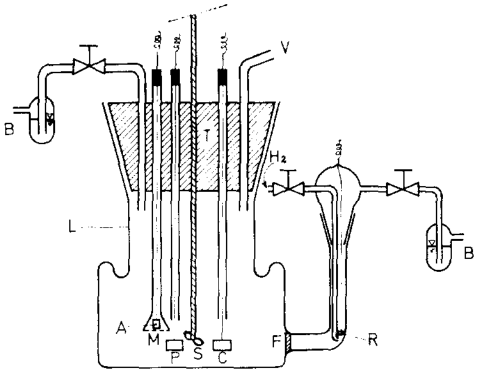

FIG. 1. The electrochemical cell. A, V, P, and R indicate, respectively, the auxiliary, collector, probe, and reference electrodes; M, cation-exchange membrane; S, stirrer; F, fritted glass; T, Teflon bung; V, connection to volumetric system; B, gas outlet through bubblers; L, solution level. Bubblers and electrode C are sketched smaller than the correct dimensions.

The aqueous electrochemical system. The experimental setup also served for some previous work (*23*), but its detailed description is given here for the first time. It consists of (i) a four-electrode electrochemical cell with a mechanical stirrer for stirring the Pd–C slurry at a variable and known speed and (ii) a gas volumeter attached to the cell and operated at atmospheric pressure.

The electrochemical cell (Fig. 1) consists of a reference electrode compartment, separated by a sintered Pyrex disk from the slurry electrode main compartment. Into this part, five glass tubes are inserted through O-ring seals. Two of the seals serve as gas inlet and outlet; through two others, gold wires are passed and sealed by picein at the top. The current collector, a gold-plate electrode (20 × 20 × 0.1 mm), and a small probe electrode, also gold, are welded to the bottom of the tubes. The fifth tube served as the auxiliary electrode compartment into which a platinum grid was inserted. It was separated from the main

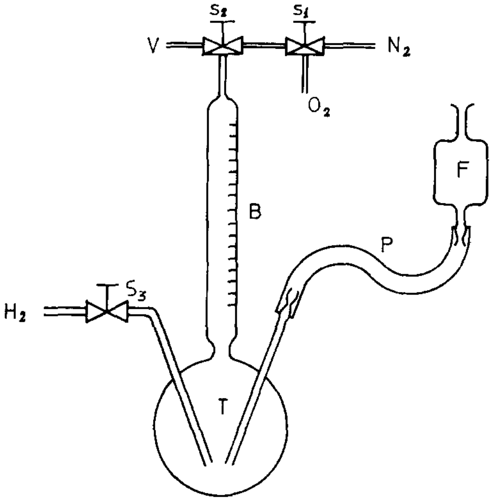

FIG. 2. The volumetric system. T, three-necked bulb; F, flask for leveling up the solution; P, tygon tube; B, burette; S, three-way valve; V, connection to electrochemical system.

cell, which contained the suspension electrode (in about 50 ml of 2 *M* H_2SO_4), by a cation-exchange membrane. This prevented excessive polarization concentration during positive discharge experiments, namely, when the auxiliary electrode was negatively charged.

The reference electrode compartment included a platinized platinum electrode, a hydrogen bubbler, and a gas outlet. The solution in both compartments was 2 *M* H_2SO_4. All electrochemical potentials, therefore, refer to a hydrogen electrode in contact with the investigated solution.

In the center of the main compartment a mechanical stirrer is passed through a mercury rotary seal. The rate of revolution was measured with a stroboscope.

Figure 2 shows the volumetric attachment. The procedure for a hydrogen adsorption experiment was as follows. The electrochemical cell was flushed first with nitrogen through the three-way valves s_1 and s_2, then with hydrogen, prewetted in bulb T, through valves s_2 and s_3 while stirring was interrupted. Under these conditions, no adsorption occurred. The solution level in the burette was brought to the starting point by raising the flask. The outlet valve of the electrochemical cell was then closed, and adsorption started immediately when stirring was begun. The elevation of the liquid level due to hydrogen uptake was measured versus time, while the solution level in the burette was continuously equalized to that in the flask by raising the latter accordingly. This was done in order to maintain constant (atmospheric) pressure.

After adsorption was complete, the cell was again flushed with nitrogen, followed by oxygen. This brought the slurry potential to its initial value of about +650 mV, which is the oxidized state. This potential, being far below that of the reversible oxygen electrode (+1.23 V), was stable upon repeated flushing with nitrogen. The setup was then ready for a new experiment of hydrogen uptake.

Curves of the double-layer charge of the carbon surface versus potential in the double-layer range were obtained by recording the probe electrode potential versus time while a constant current was passed between the collector and the auxiliary electrodes. The solution was constantly stirred under nitrogen atmosphere. Upon stirring, the Pd–C particles colliding with the collector accepted practically all the electrical charge supplied by the galvanostat [Figs. 4 and 5 in Ref. (*23*)].

In order to keep the collector electrode potential within the double-layer range,[3] the applied constant currents were never higher than a few milliamperes.

The solid–gas system. Hydrogen adsorption on dry carbon was carried out in a conventional Pyrex vacuum system. For

---

[3] The double-layer range of potentials in aqueous 2 *M* H_2SO_4 solution extends between the potentials of hydrogen and oxygen solution reactions. With the hydrogen reference electrode in the same solution used here, this range is between 0.00 and 1.23 V. Within it, inert and noncatalytic electrodes, such as gold and carbon, behave as ideally polarized electrodes (*24*), namely, the entire charge is utilized for double-layer charging.

evacuation down to 10^{-6} Torr, an oil-diffusion pump, backed by a dual-stage rotary van pump, was used. The vacuum was monitored with McLeod and Pirani gauges. High temperatures were attained by portable laboratory-made small ovens and Eurotherm thermocouple temperature controllers.

Hydrogen adsorption pressures were measured using a differential constant-volume mercury manometer and a cathetometer of 10^{-2}-mm resolution. For each adsorption experiment, a single dose of hydrogen was used at a pressure of 380–480 Torr measured by the cathetometer. Adsorption was followed by reading the pressure drop in the constant volume system. The final pressure was never lower than 250 Torr.

Prior to adsorption experiments, the samples were evacuated for 2 hr at 550°C, which was the highest adsorption temperature applied. This procedure is known to result in partial exclusion of surface oxides, mainly as CO_2 (*15*). Each sample was used only once in the hydrogen chemisorption experiments since desorption was impossible at 550°C.

Nitrogen for BET surface measurements was passed through a cold trap (−195°C) filled with glass beads to remove traces of water and was stored before use in glass bulbs. High-purity hydrogen was obtained by the thermal decomposition of uranium trihydride. Hydrogen pressures up to 1 atm were obtained by heating the hydride to 450°C. The hydride had been previously prepared or regenerated by reacting hydrogen (Ultra Pure, Matheson) on uranium shavings (Fluka).

All experiments with the slurry electrode were performed in 2 *M* H_2SO_4 at room temperature (23–26°C).

RESULTS

Figure 3 is a typical plot of the amount of hydrogen adsorbed on Pd/C versus time at different stirring rates. The final quantity largely exceeds that absorbed by palladium alone (*26*), whereas the ratio H/Pd is 0.6 at room temperature and under atmospheric pressure.

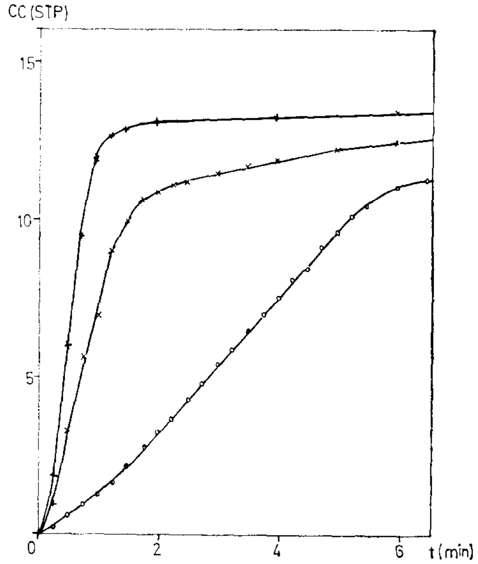

FIG. 3. Hydrogen uptake by 1 g of 1% palladized carbon vs time. Stirrer speeds are: (○) 1500 rpm; (×) 2100 rpm; (+) 3000 rpm.

The data in Fig. 4 enables us to obtain the hydrogen consumption by Pd alone by two different means. The 0.43 ml (STP) of the final uptake by 1.5 mg of palladium is equal to the difference in uptake of two samples containing 1 and 2.5 mg of Pd in 0.1 g of carbon. Since palladium was introduced as $PdSO_4$ prior to H_2 admission, a calculated amount of 0.41 ml (STP) of hydrogen should have been consumed by 1.5 mg of Pd to give a Pd/H ratio of 0.6 (*26*). This value is in agreement with the measured value of 0.43 ml.

Figure 5 shows this excess adsorption on carbon, together with a curve obtained with a carbon sample which was added to an already hydrogenated palladium–carbon powder. Measurements with different combinations of carbon and palladium gave reproducible results of the net amount adsorbed on carbon, 10.6 ml (STP) of H_2/g of carbon (870 m^2/g of BET surface area). In the absence of palladium, carbon does not absorb hydrogen at room tem-

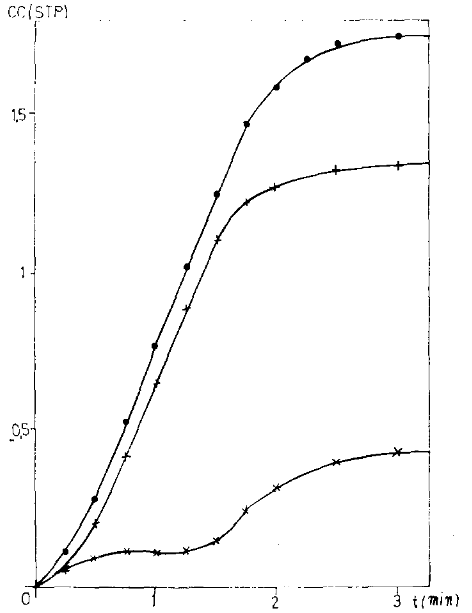

FIG. 4. Hydrogen uptake by: (●) 100 mg of carbon with 2.5 mg of palladium; (+) 100 mg of carbon with 1 mg of palladium; (×) 1.5 mg of palladium.

perature. This was established both in the acid slurry and in the solid–gas system.

The delay in adsorption for the Pd/C powder resulted from the correction for uptake by Pd, which was arbitrarily assumed to be complete before adsorption on carbon.

Anodic and cathodic charging was carried out under nitrogen atmosphere. The curves obtained are given together with curves of hydrogen uptake, expressed in coulombs, versus potential (Fig. 6). All results are at room temperature. The quantitative agreement, especially of the total amount, indicates that both electrical charging of carbon powder and hydrogen uptake are essentially the same process.

In Fig. 7 the hydrogen uptake is given versus time for three experiments with 1 g of 1% Pd/C soaked in 0.5 ml of water, 10^{-4} M H_2SO_4, and 2 M H_2SO_4, respectively. This restricted quantity of liquid amounts to about two monolayers if spread evenly on the carbon surface. The rates of adsorption and the final amounts adsorbed are similar, within the experimental error.

Figure 8 presents curves of adsorption versus time at several high temperatures without preadsorbed water. This does not imply, however, that water is completely absent, since part of the surface carbon oxides may be reduced by hydrogen to give water. It seems unlikely that a significant

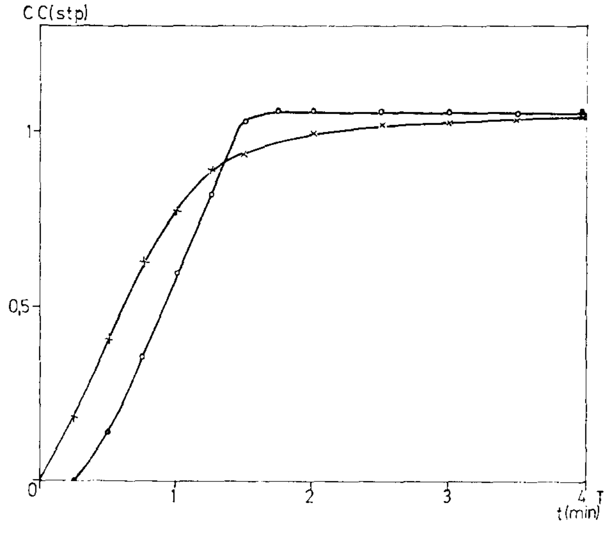

FIG. 5. Hydrogen uptake by 100 mg of 1% palladized carbon (○), followed by uptake by the 100 mg of pure carbon (+) added to the previously hydrogenated slurry.

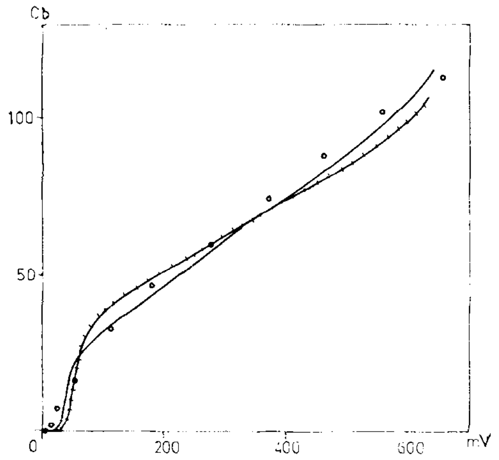

FIG. 6. Anodic (——) and cathodic (- - - -) charging curves under nitrogen atmosphere, and amount of hydrogen uptake (○) vs potential at open circuit on 1 g of 1% palladized carbon suspension in 2 *M* H_2SO_4. Direct hydrogen uptake is converted to coulombs (1 mmole ≡ 193 C). For further details, see Experimental.

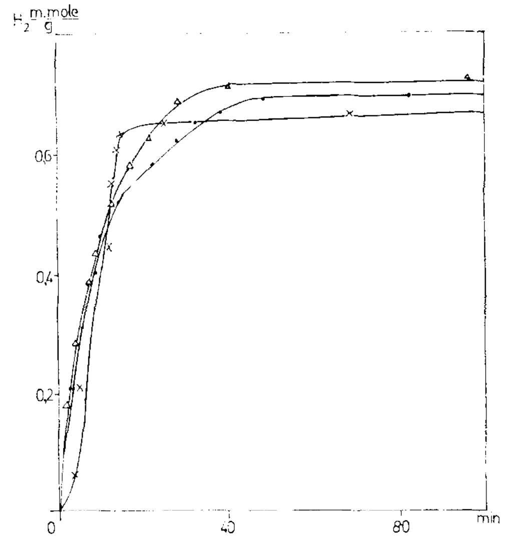

FIG. 7. Hydrogen uptake on 1 g of 1% palladized carbon to which 0.5 cm³ of triple-distilled water is added; (●) 10^{-4} *M* H_2SO_4; (×) 2 *M* H_2SO_4.

fraction of the hydrogen uptake is due to palladium (10 weight%) since, at temperatures above 150°C and at the pressure range employed, hydrogen absorption amounts to an H/Pd ratio of at most 0.05 (*27*) on bulk Pd, which corresponds to only 2.5×10^{-3} mmole of H_2/g of 10% Pd on carbon. One could argue, on the other hand, that our samples contain highly dispersed Pd in which the H/Pd ratio may approach unity, as for Pt (*15*). If this were true, the rate of uptake would be several orders of magnitude faster than the rate at the much

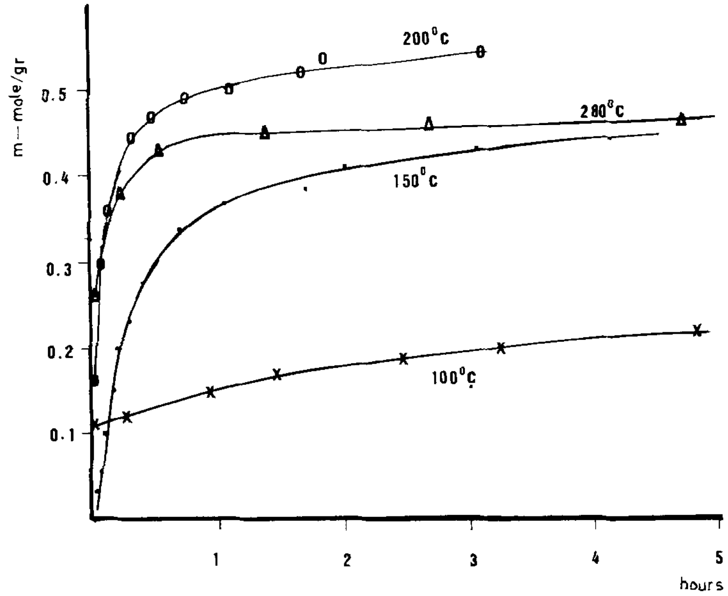

FIG. 8. Hydrogen adsorption on 10% palladized carbon at various temperatures.

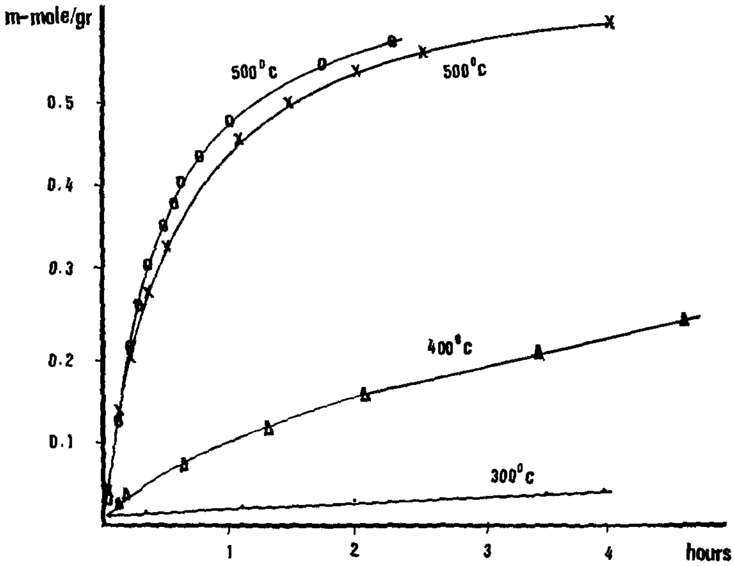

FIG. 9. Hydrogen adsorption on pure carbon at various temperatures.

lower room temperature (Figs. 3–5). A contrary behavior is exhibited by experiment.

The slightly higher uptake at 200°C as compared to that at 260°C can be attributed to either high experimental error or to restrictions of the co-catalyst function (*20*) of water produced by surface oxide reduction, but desorbed at the higher temperature.

Hydrogen chemisorption on pure carbon commences only at temperatures higher than that of palladized carbon, as is shown in Fig. 9. This difference clearly demonstrates the catalytic effect of palladium, i.e., the *spillover* of hydrogen from Pd onto the carbon support.

The series of solid–gas experiments lacked the reproducibility needed for obtaining Arrhenius plots and activation energies for the appropriate rate-determining steps.

The behavior of carbon as seen in Figs. 7–9 resembles that of tungsten trioxide under similar conditions (*6*).

In Table 1, the final hydrogen uptake or the variations in double-layer charging are given together with other related magnitudes for six types of experiments. The magnitudes obtained for the various experimental conditions are very similar.

DISCUSSION

Pd/C Slurry in Solution

The absence of uptake of hydrogen by the carbon slurry, the net uptake on carbon in the presence of palladium (Fig. 3), and the conjugated shift of the slurry electrode potential (Fig. 6) have already been explained by electrochemical concepts (*23*). A Pd particle has the same electrochemical potential as a carbon particle when they are in contact. This potential is initially +650 mV versus a hydrogen electrode in the same solution.[4] Dissolved hydrogen molecules are catalytically adsorbed on Pd and are dissociated according to the overall reaction,

$$\tfrac{1}{2}\mathrm{H}_2 \rightarrow \mathrm{H}_{\mathrm{aq}}{}^{+} + e_{\mathrm{M}}. \qquad (1)$$

This reaction proceeds until the Pd particle attains zero potential due to the accumulating electronic charge, e_M, on the metal side of the interface.

The carbon particles also follow this potential change after impacts between Pd

---

[4] This initial potential results from prolonged exposure of wet Pd–C powder to air. The oxygen electrode potential (~1.2 V) might be achieved if the mixture behaved as a reversible O_2 electrode.

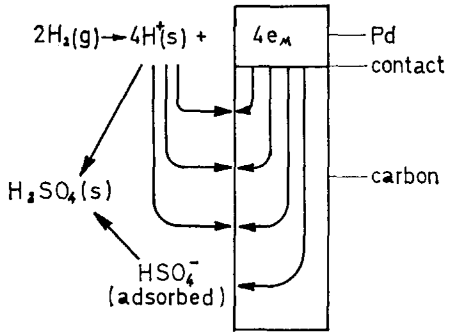

FIG. 10. Electrochemical presentation of hydrogen uptake by carbon, in contact with Pd catalyst.

and C particles. Since no redox reaction exists in H_2SO_4 solution in the range of potentials considered, the only negative charge acquired by the active carbon is that for the double-layer (dl) potential change (from +650 to 0 mV). The term dl change also stands for surface group reactions and specific adsorption. Obeying the electroneutrality condition, the increase in negative electronic charge must be compensated for by some desorption of HSO_4^- and probably also of SO_4^{2-} ions and adsorption of H^+ ions. The overall process can be described by the following equation:

$$\tfrac{1}{2}n\mathrm{H}_2 + \begin{array}{c|l} & (n-x)\mathrm{HSO}_4^- \\ \mathrm{M} & \mathrm{S} \end{array} \rightarrow \begin{array}{c|l} ne & x\mathrm{H}^+ + (n-x)\mathrm{HSO}_4^- + (n-x)\mathrm{H}^+ \\ \mathrm{M} & \mathrm{S} \end{array} . \qquad (2)$$

The symbol M|S stands for the metal–solution interface with the indicated adsorbed species. It can be seen from Eq. (2) that, provided a mobile and adsorbable anion exists, it is unnecessary that all the n equivalents of gaseous hydrogen consumed be adsorbed, but, rather, a part $n - x$ $(0 \leqslant x \leqslant 1)$ of it is liberated, together with the desorbed anion, as a free acid. This is the reason we use the general term "uptake" of hydrogen rather than adsorption in the slurry system.

The transport of the different species involved in dl charging of the carbon surface is schematically shown in Fig. 10. Four steps of transport can be observed, each of which might be the rate-determining step (rds). These are: (i) The catalytic dissociation of H_2 into hydrated protons and metal conduction band electrons [Eq. (1)]; (ii) the transfer of electrons through the electronic contact between Pd and support; (iii) the electronic conduction of the support; (iv) the ionic conductivity of the electrolyte. Steps i, ii, and iii are consecutive while step iv is parallel to ii and iii.

Prior to these steps are: (a) dissolution of molecular hydrogen into the bulk of the electrolyte and (b) diffusion of H_2 across a diffusion layer surrounding the Pd particle. It is shown in Fig. 3 that, under the present experimental conditions, stage a is the rds for the slurry systems. More details about the kinetics of H_2 uptake by Pd–C slurry are given in Ref. (*23*). Stage a is not applicable to the solid–gas spillover system, while stage b can still apply if water vapor in equilibrium with preadsorbed water surrounds the sample, since hydrogen at low pressure must diffuse through the vapor phase.

Let us now imagine that the Pd–C point of contact in Fig. 11 is replaced by metallic lead of variable resistivity, which protrudes from the solution to enable electrical measurements. Since no direct hydrogen uptake is possible by the pure noncatalytic carbon, a conventional electrochemical cell is now obtained (Fig. 1), by which the negative

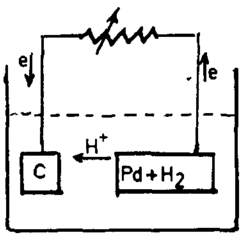

FIG. 11. Equivalent electrochemical cell for the Pd–C electrolyte.

hydrogen (Pd) electrode supplies protons and electrons to the more positive carbon. Thereby, it probably reduses functional groups of the surface (*28*) by some specific surface hydrogenation or hydrogen chemisorption and also positively charges its ionic diffuse dl.

The redox properties of surface groups of carbon have been extensively studied by Frumkin *et al.* (*29*) and by Garten *et al.* (*30*). The many different carbons used, as well as the presented consequences, are rather confusing. However, a thorough study of the significance of the double-layer charge (*31*) and a recent paper on generalized dl thermodynamics of reversible electrodes (*28*) show that all the chemical changes which involve adsorbed species can be interpreted in terms of the simple ideally polarized electrode thermodynamics of chemically inert species. Applying the essence of those studies to our immediate purpose, we can easily observe from Fig. 10 that the overall process of hydrogen transfer (or spillover) from Pd to the C surface is electrochemically completed without the need to specify *how* the hydrogen is bonded to the surface. Therefore, the macroscopic observation of hydrogen uptake is sufficiently explained in terms of the generalized dl charging which includes any type of surface hydrogenation or reduction. It can easily be seen that this approach is applicable to hydrogen spillover and chemisorption in the solid–gas system as well.

Returning now to the imaginary electrochemical cell of Fig. 11, it can be seen that the driving force for the transport of both electrons and ions is the electric field. This is self-evident for electrons in the lead. This can be readily understood for ions by assuming that the rds is the ohmic conduction of the solution; the whole initial potential difference of 650 mV, then, falls across the solution. The importance of this driving force will be stressed in a subsequent publication on hydrogen spillover on tungsten trioxide.

The dl interpretation of hydrogen spillover over carbon in solution is further supported by the agreement between the integral capacity calculated from hydrogen uptake versus potential and that obtained from the anodic and cathodic charge curves given in Fig. 7. In Table 1 the four values of dl capacity are presented: Three of them are integral. The value of 17 μF/cm^2 is characteristic of a mercury double-layer system (*24*) without specific adsorption. However, it has been found that the dl capacity of carbon is 9–11 μF/cm^2 in about the same potential range for NaCl solution (*32, 33*). Since sulfate ions are known to exhibit less specific adsorption than chloride (*24*), one must conclude that specific

TABLE 1

Hydrogen Uptake, Double-Layer Charge, and Related Magnitudes[a]

Type of experiment	mmole/g	μC/cm^2	Coverage ($\sigma \times 10^2$)	Integral dl capacity (μF/cm)
H_2 on slurry of Pd/C	(0.55)	12.6	3.7	19.5
Anodic charging	0.56	(13.2)	3.8	20
Cathodic charging	0.55	(12.6)	3.7	19.5
H_2 on wet Pd/C	(0.63)	14.5	4.0	
H_2 on Pd/C at 200°C	(0.55)	12.6	3.7	
H_2 on pure C at 200°C	(0.6)	13.8	4.15	

[a] Numbers in parentheses were obtained directly from experiments; others were calculated using a BET surface area of 870 m^2/g and an H_2 site area of 10 Å^2.

adsorption of protons exists on carbon in contact with acid solution.

Room-Temperature Adsorption on Wet Pd/C Powder

This is an intermediate between the electrochemical system described above, for which the spillover mechanism is shown to be simple double-layer charging, and the solid–gas system, where the spillover phenomenon is not yet clearly understood.

Figure 7 shows that hydrogen spillover (in the pressure range of 250–480 Torr) on the wet powder is, though still rapid, about one order of magnitude slower than on the suspension electrode. This difference in rates stimulates some questions about the role of the various transport states in the two adsorption systems described.

The very first step of hydrogen dissolution into the liquid phase containing the suspension electrode does not exist for the wet powder because of the easy access of hydrogen gas to the pores between the nonflooded particles. This step, however, was found to be the rds in the suspension electrode (*23*). The conduction of electrolyte is doubtless much lower for the wet powder, but this limited conduction is not the rds, since the conduction of the three wetting solutions differs greatly, while the rate of H_2 uptake is about the same (Fig. 7). A possible but not unambiguous rds is the diffusion of hydrogen through the (static) liquid layer. The limited conduction may still be the rds if the Pd/C powder already contains adsorbed H_2SO_4 in an amount comparable to that introduced by adding 0.5 ml of 2 *M* acid.

No matter which is the rds for hydrogen uptake by the wet powder, the great similarity to the suspended Pd/C (electrochemical) system is clear, and hydrogen spillover occurs at room temperature if water or electrolytic solution are admitted to an amount of approximately two monolayers only.

The Solid–Gas System without Preadsorbed Water

It is now obvious that, by gradually decreasing the amount of preadsorbed water by high-temperature evacuation, ionic conduction of the "electrolyte" will sooner or later be the rate-determining step. Higher temperatures will be necessary to enhance this conduction and allow measurable spillover. This is described in Fig. 8 where it is shown that relatively slow hydrogen adsorption on carbon proceeds by palladium activation.

The mechanism now proposed (though not proved) for the solid–gas system is that molecular hydrogen is dissociated to electrons and protons. These species migrate through the solid conduction band and the surface hydroxyl groups, respectively, to chemisorption sites much farther from the palladium particles. The conduction on the dry carbon surface is supposed to proceed through hydrogen bonds bridging the hydroxy surface groups, which undoubtedly exist in the form of several functional groups (*34*).

The ionic conduction through hydroxyls via hydrogen bonds is well known for silica (*35*, *36*), silica–alumina (*37*), and borax (*38*). It generally increases upon adsorption of protonic molecules (*35*, *36*). It is detected relatively easily when no electronic conduction exists at the same time. It presumably exists on every surface which contains hydroxyl groups, or adsorbed water, or both. In the latter case, adsorbed water increases the surface density of the H-bond bridges between surface hydroxyls (*38*). Unfortunately, it is almost impossible to detect directly ionic conduction on surfaces of carbons, graphites, or metals,. due to the interference of the immensely higher electronic conductance.

Expected Properties of Spillover Systems in the Light of the dl Mechanism

(i) The driving force for the transport of active species is the electrical potential gradient between the catalyst and the reactive site on the support remote from the catalyst. It is this driving force which might be responsible for the very high rate of hydrogenation of tungsten trioxide observed (*6*, *20*). This property is in complete analogy with ionic and electronic transport in ordinary electrochemical cells (Figs. 10 and 11), whereas the surface OH groups and adsorbed water or other hydrogen bonding molecules (*20*) serve as electrolyte.

(ii) As an ionic–protonic transport between two "electrodes," spillover is a long-range macroscopic process. It may extend to visible distances, as has been observed by Benson for tungsten trioxide (*39*) and by Bianchi *et al.* for aerogel alumina (*14*) and as demonstrated in Fig. 5, which shows that hydrogen uptake proceeds on pure carbon slurry if added to Pd/C. Sancier (*7*) calculated, though he did not directly observe, a spillover distance of about 0.5 mm for hydrogen on alumina. Such long ranges of transport of active hydrogen can hardly be explained if the "active species" is unstable [H_3O radical (*6*) or the like].

(iii) Considering the above discussion, it is obvious that the combination of both ionic and electronic conduction of the support is a condition for the mechanism proposed. Surface ionic conductivity can always be assured if a sufficient density of surface OH groups and/or adsorbed hydrogen bonding molecules is present. Electronic (bulk) conductance, on the other hand, is known to exist in many of the transition-metal oxides possessing slight nonstoichiometry or crystal defects. Outstanding in high electronic conductivity are the oxide bronzes, a group of nonstoichiometric substances, to which tungsten trioxide (*19*) also belongs, if partially reduced by hydrogen or other reducing agents.

In this respect, spillover of hydrogen on alumina is not surprising, since hydrogen adsorption by γ- and η-aluminas was observed by Weller and Montague (*40*) at 200–500°C and by Amenomiya (*41*) at both high and low temperatures. Evidence of nonstoichiometric aluminas was reported by Hoang–Van and Teichner (*42*) and by Literat (*43*). Moreover, *n*-type electronic semiconductor properties were found upon exposure of η-alumina to hydrogen at 600°C (*44*).

(iv) The amount of hydrogen uptake must correlate with the capacity of the double layer existing on every solid–gas interface. (This double layer is at equilibrium wherever electronic and ionic conduction exist simultaneously.) This aspect, which, again, is self-evident for the electrode–solution interface, provides an explanation for the limited coverage of chemisorbed hydrogen from the gaseous phase which amounts to only a few hundredths of a monolayer (Table 1, see also Ref. (*9*)]. This limited amount is simply the amount necessary to charge the dl in either the liquid or gaseous phase. In fact, it is shown in Table 1 that the hydrogen uptake by the slurry electrode is in good agreement with the amount of dl charge which changes the carbon powder potential from +650 to 0 mV. Regarding the solid–gas experiments, one might expect some discrepancies in the amount of H_2 uptake, as compared to that from solution. This is because of an expected change in dl capacity at high temperatures and of the rarified "electrolyte." Also, the initial potential may be different from the +650 mV observed for the slurry electrode. However, Table 2 also shows good agreement between H_2 uptake from the gaseous phase and that from solution.

We believe that this coincidence results from compensating shifts in the properties of the interface upon changing from the liquid to the gaseous phase at higher temperatures.

One would expect that, if the initial carbon potential is closer to the final 0 mV versus the H_2 electrode, the hydrogen uptake would be lower. Reducing the surface oxides (or surface positive dipoles) of carbon by high-temperature treatment, as done by Boudart *et al.* (*3*), should cause this potential shift to result in a much lower H_2 chemisorption. In fact, it has been shown (*32*) that high temperature evacuated carbon resulted in a 350-mV negative shift in its initial potential when immersed in a dilute NaCl solution.

REFERENCES

1. Sinfelt, J. H., and Lucchesi, P. J., *J. Amer. Chem. Soc.* **85**, 3365 (1963).
2. Robell, A. J., Ballou, E.V., and Boudart, M., *J. Phys. Chem.* **68**, 2748 (1964).
3. Boudart, M., Aldag, A. W., and Vannice, M. A., *J. Catal.* **18**, 46 (1970).
4. Suzuki, S., and Suzuki, T., *Bull. Chem. Soc. Japan* **38**, 2020 (1965).
5. Khoobiar, S., *J. Phys. Chem.* **68**, 411 (1964).
6. Benson, J. E., Kohn, H. W., and Boudart, M., *J. Catal.* **5**, 307 (1966).
7. Sancier, K. M., *J. Catal.* **23**, 298 (1971).
8. Boudart, M., Vannice, M. A., and Benson, J. E., *Z. Phys. Chem.* **64**, 171 (1969).
9. Nowak, E. J., *J. Phys. Chem.* **73**, 3790 (1969).
10. Il'chenko, N. I., *Kinet. Katal.* **8**, 184 (1967) (English trans.).
11. Bond, G. C., Sermon, P. A., and Tripathi, J. B. P., *Ind. Chim. Belg.* **38**, 506 (1973).
12. Ekstrom, A., Batley, G. E., and Johnson, P. A., *J. Catal.* **34**, 106 (1974).
13. Batley, G. E., Ekstrom, A., and Johnson, P. A., *J. Catal.* **34**, 368 (1974).
14. Bianchi, D., Gardes, G. E. E., Pajonk, G. M., and Teichner, S. J., *J. Catal.* **38**, 135 (1975).
15. Sermon, P. A., and Bond, G. C., *Catal. Rev.* **8**, 211 (1973).
16. Neikam, W. C., and Vannice, M. A., in "Proceedings of the 5th International Congress on Catalysis," Vol. 1, p. 609. North-Holland, Amsterdam, 1973.
17. Vannice, M. A., and Neikam, W. C., *J. Catal.* **20**, 260 (1971).
18. Neikam, W. C., and Vannice, M. A., *J. Catal.* **27**, 207 (1972).
19. Hobbs, B. S., and Tseung, A. C. C., *J. Electrochem. Soc.* **119**, 580 (1972).
20. Levy, R. B., and Boudart, M., *J. Catal.* **32**, 304 (1974).
21. Stonehart, P., and Ross, P. M., *Catal. Rev. Sci. Eng.* **12**, 1 (1975).
22. Stoffer, A., *J. Electroanal. Chem.* **40**, 153 (1972).
23. Keren, E., and Soffer, A., *J. Electroanal. Chem.* **44**, 53 (1973).
24. Grahame, D. C., *Chem. Rev.* **41**, 441 (1947).
25. Barton, S. S., *Carbon II*, 649 (1973); *Discuss. Faraday Soc.* 1039 (1973).
26. Lewis, F. A., "The Palladium-Hydrogen System." Academic Press, London, 1967.
27. Scholten, J. J. F., and Konvalinka, J. A., *J. Catal.* **5**, 1 (1966).
28. Garten, V. A., and Weiss, D. E., *Aust. J. Chem.* **10**, 309 (1957).
29. Frumkin, A. N. et al., *Acta Physicochim. SSSR* **12**, 795 (1940).
30. Garten, V. A., Weiss, D. E., and Willis, J. B., *Aust. J. Chem.* **10**, 295 (1957); Garten, V. A., and Weiss, D. E., *Rev. Pure Appl. Chem.* **7**, 69 (1957).
31. Frumkin, A. N., Petrii, O. S., and Damaskin, B. B., *J. Electroanal. Chem.* **27**, 81 (1970).
32. Soffer, A., and Folman, M., *J. Electroanal. Chem.* **38**, 25 (1971).
33. Yaniv, M., Master of Science thesis, Feinberg Graduate School, The Weizmann Institute of Science, Rehovot, Israel (1974).
34. Donnet, J. B., *Carbon* **6**, 161 (1968).
35. Levy, S., and Folman, M., *J. Phys. Chem.* **67**, 1278 (1963).
36. Soffer, A., and Folman, M., *Trans. Faraday Soc.* **62**, 3559 (1966).
37. Voltz, E. E., and Weller, S. W., *J. Phys. Chem.* **62**, 576 (1958).
38. Maricic, S., Pintar, M., and Velski, Z., *J. Phys. Chem. Solids* **23**, 743 (1962).
39. Benson, J. E., unpublished data [cf. Ref. (*20*)].
40. Weller, S. W., and Montagna, A. A., *J. Catal.* **21**, 303 (1971).
41. Amenomiya, Y., *J. Catal.* **22**, 109 (1971).
42. Hoang-Van, C., and Teichner, S. J., *J. Catal.* **16**, 69 (1970).
43. Literat, L., *Rev. Roum. Chim.* **13**, 731 (1968).
44. Khoobiar, S., Carter, J. L., and Lucchesi, P. J., *J. Phys. Chem.* **72**, 1682 (1968).